The Higgs mass in the MSSM infrared fixed point scenario[*]

J.A. Casas[¶], J.R. Espinosa[†] and H.E. Haber[§]

[¶] Instituto de Estructura de la Materia, CSIC

Serrano 123, 28006 Madrid, Spain

casas@cc.csic.es

[†] CERN, TH Division

CH-1211 Geneva 23, Switzerland

espinosa@mail.cern.ch

[§] Santa Cruz Institute for Particle Physics

University of California, Santa Cruz, CA 95064, USA

haber@scipp.ucsc.edu

Abstract

In the infrared fixed point (IFP) scenario of the minimal supersymmetric model (MSSM), the top-quark mass and other physical quantities of the low-energy theory are insensitive to the values of the parameters of the theory at some high energy scale. In this framework we evaluate the light CP-even Higgs mass, m_{h^0}, taking into account some important effects that had not been previously considered. In particular, the supersymmetric correction to the relation between the running and the physical top-quark masses lowers the value of $\tan\beta$, thereby implying a lower predicted value of m_{h^0}. Assuming a supersymmetric threshold of $M_S \leq 1$ TeV and $M_t = 175$ GeV, we find an upper bound of $m_{h^0} \leq 97 \pm 2$ GeV; the most plausible value of m_{h^0} lies somewhat below the upper bound. This places the Higgs boson in the IFP scenario well within the reach of the LEP-2 Higgs search.

1   Introduction

Models of low-energy supersymmetry can add many new parameters to the Standard Model. The minimal supersymmetric extension of the Standard Model (MSSM) is minimal only in its choice of particle content. The number of free parameters of the model is quite large unless additional theoretical assumptions are imposed. The parameter freedom of the MSSM is due mostly to soft supersymmetry-breaking parameters, whose theoretical origins are unknown. It is common practice to treat the parameters of the MSSM as running parameters and impose a particular structure on the soft supersymmetry breaking terms at a common high energy scale [such as the Planck scale ($M_{\rm P}$) or grand unification (GUT) scale (M_X)]. Using the renormalization group equations (RGEs), one can then derive the values of the low-energy MSSM parameters.

A particularly attractive framework, which we will adopt in this paper, consists of assuming universality of soft breaking parameters at the high-energy unifying scale. Universality is a desirable property not only to reduce the number of independent model parameters, but also to avoid unsuppressed flavor changing neutral currents (FCNCs) [1]. Universality of scalar and gaugino mass parameters in the high energy theory is an automatic consequence of the *minimal* supergravity (SUGRA) framework [2] and approximately holds in several string-derived SUGRA scenarios [3].

The resulting low-energy supersymmetric theory that emerges depends on five supersymmetric model parameters: a common scalar mass m, a common gaugino mass M, a common flavor-diagonal trilinear scalar coupling A, a supersymmetric Higgs mass parameter μ, and an off-diagonal Higgs squared-mass parameter m_{12}^2 (often called $B\mu$). These parameters are high-energy scale parameters (defined at either $M_{\rm X}$ or $M_{\rm P}$) and serve as initial conditions for the RGEs. Electroweak symmetry breaking in the low-energy theory is radiatively generated when one of the Higgs squared-masses is driven negative by renormalization group (RG) running. Then, by imposing the minimum conditions for the Higgs potential, one can eliminate μ^2 and m_{12}^2 in favor of the electroweak symmetry-breaking scale, $v^2 \equiv v_1^2 + v_2^2 \simeq (174 \text{ GeV})^2$, and $\tan\beta \equiv v_2/v_1$, where v_1 and v_2 are the Higgs vacuum expectation values. The sign of μ is not fixed in this procedure and remains a free parameter.

Clearly, the previously described SUGRA theory is a highly constrained version of the MSSM. Nevertheless, there can be additional interesting constraints. In particular, certain low-energy MSSM parameters are sometimes very insensitive to the initial high energy values of the SUGRA parameters. Such a possibility is very exciting, since it offers a potential for understanding the physical value of some low-energy parameters without a detailed knowledge of the physics at high energies.

The classic example of the scenario just described is the quasi-infrared fixed point (IFP) prediction for the top-quark Yukawa coupling [4,5,6,7,8,9,10,11,12,13,14,15][1]. As

---

[1]The quasi-infrared fixed point differs from the infrared fixed point of Pendleton and Ross (PR)[16]. The PR fixed point is an infrared stable fixed point that is reached at a scale Q for sufficiently large M_X/Q. However, in practice M_X/m_Z is not large enough, so the PR fixed point solution does not govern the low-energy value of the top-quark Yukawa coupling. On the other hand, it follows from eqs. (1)–(3) that the top-quark Yukawa coupling is driven to the quasi-infrared fixed point as long as $Y_t(0)F(t_Z) \gg 1/6$, where $t_Z \equiv \ln(M_X^2/m_Z^2)$.

is well known [5], the one-loop RGE of the top-quark Yukawa coupling, $Y_t \equiv h_t^2/(4\pi)^2$, can be integrated analytically for moderate values of $\tan\beta \sim \mathcal{O}(1)$:

$$Y_t(t) = \frac{Y_t(0)E(t)}{1 + 6Y_t(0)F(t)}, \tag{1}$$

with

$$E(t) = (1 + \beta_3 t)^{16/3b_3}(1 + \beta_2 t)^{3/b_2}(1 + \beta_1 t)^{13/9b_1} \ , \quad F(t) = \int_0^t E(t')dt' \ . \tag{2}$$

In eq. (2), $\beta_i \equiv \alpha_i(0)b_i/4\pi$ are the one-loop beta functions of the gauge couplings $\alpha_i(t)$, with $(b_1, b_2, b_3) = (11, 1, -3)$, and $t = \ln(M_X^2/Q^2)$, where Q is the renormalization scale. This one-loop behavior leads to the existence of the quasi-infrared fixed point. Namely, for $Y_t(0) \to \infty$,

$$Y_t(t) \to Y_f(t) \equiv \frac{E(t)}{6F(t)}. \tag{3}$$

Numerically, one finds that Y_t at the electroweak scale differs negligibly from Y_f for a wide range of $Y_t(0) \gtrsim 0.01$, so in this sense the low-energy value of Y_t is indeed insensitive to its high-energy value $Y_t(0)$. The value of the top-quark mass depends both on the low-energy values of Y_t and $\tan\beta$, so at this stage we do not have a prediction for the top-quark mass. Nevertheless, the parameter freedom has been reduced, since given the top-quark mass, $\tan\beta$ is now predicted. Actually, $\tan\beta$ typically turns out to be near 1, in which case the previous derivation is fully justified[2].

In this paper, we focus on the prediction of the light CP-even Higgs mass (m_{h^0}) in the IFP scenario as a function of the minimal SUGRA parameters. We improve on previous work in the literature by taking into account a number of effects not fully considered before. These include: (i) corrections to $\tan\beta$ due to supersymmetric thresholds; (ii) evolution of $\tan\beta$ from the electroweak scale to the supersymmetry-breaking scale; and (iii) a precise evaluation of radiative electroweak breaking and of the top-squark (stop) mixing parameter. All these effects have a significant impact on the value of m_{h^0}. In addition, we have computed m_{h^0} using the most refined methods available, including subdominant radiative corrections and contributions from stop non-degeneracy. This substantially reduces the theoretical uncertainty of our results with respect to previous literature. Our final result on the upper bound on the Higgs mass has important implications for the LEP-2 Higgs search.

In Section 2, we discuss the IFP scenario and the calculation of $\tan\beta$, as well as the stop mixing parameter, including all the new effects mentioned above. We address a number of effects not previously considered, which can significantly affect the predicted value of $\tan\beta$ and the Higgs mass. In Section 3, we review the dependence of the Higgs mass on the supersymmetric parameters. In Section 4, we explore the consequences of the IFP scenario for the predicted value of the Higgs mass, giving full numerical results and comparing to the previous literature. Conclusions are presented in Section 5.

---

[2] If one solves the complete set of RGEs for the top and bottom-quark Yukawa couplings, one finds another IFP solution with $\tan\beta \sim m_t/m_b$. In this paper, we will not address this large $\tan\beta$ scenario since, in the minimal SUGRA approach described above, it requires a precise (unnatural) fine-tuning of high-energy parameters in order to ensure the correct radiative electroweak symmetry breaking [17].

2 The IFP scenario revisited

In Section 1, we reviewed the quasi-infrared fixed point (IFP) scenario in which the low-energy value of the top-quark Higgs Yukawa coupling is driven to a quasi-infrared fixed point value, Y_f. Formally, this limit is derived by taking $Y_t(0) \to \infty$. This is not theoretically consistent as it stands, since the derivation given above was based on a one-loop RGE, while large values of $Y_t(0)$ clearly lie outside the perturbative regime. However, it has been shown [18] that the domain of attraction of the quasi-IFP is large and accurately represented by the one-loop approximation. In particular, $Y_t(0)$ rapidly approaches Y_f, even for values of $Y_t(0)$ still in the perturbative region. This allows one to consider the IFP limit as a meaningful physical possibility. For example, starting with $Y_t(0) = 0.1$ the one-loop value of $Y_t(t)$ at the weak scale differs from Y_f by 0.27%. In this paper, we employ two-loop RGEs for the evolution of the gauge and Yukawa couplings. For definiteness, we choose $Y_t(0) = 0.1$, although the results are insensitive to this choice, as argued above.

Another subtlety concerning the precise definition of the IFP scenario is the choice of the unification scale M_X and of $\alpha_i(0)$. Here, we follow the approach of Ref. [19]. First, we take the experimental values of $\alpha_i(Q = m_Z)$ as input parameters and evaluate the corresponding supersymmetric $\overline{\text{DR}}$ values, $\hat{\alpha}_i(m_Z)$, taking into account all the supersymmetric threshold corrections[3] [the $\hat{\alpha}_i(m_Z)$ do not have a direct physical meaning; see Ref. [19] for more details]. Then, the two-loop running of $\hat{\alpha}_1(t)$, $\hat{\alpha}_2(t)$ to high scales defines a unification scale M_X and a "unified" coupling constant $\hat{\alpha}(0)$. Finally, the running of $\hat{\alpha}_3$ from m_Z to M_X gives the value of $\hat{\alpha}_3(0)$. In general, the latter does not coincide (even within the error bars) with $\hat{\alpha}(0)$, although the difference is small and can be attributed to, for instance, threshold corrections either from a GUT or stringy origin.

The IFP scenario defined in the context of the SUGRA approach depends on additional parameters m, M, A, $\tan\beta$ and $\text{sign}(\mu)$ as described in Section 1. However, the subset of independent parameters is substantially smaller. In the IFP scenario, the low-energy value of A_t (the trilinear scalar coupling of the Higgs boson and stops) is also driven to an infrared quasi-fixed point [7]. At the one-loop level

$$A_t(t) \to M \left[\frac{1}{4\pi} \left(\frac{16}{3} \alpha_3(0) h_3 + 3\alpha_2(0) h_2 + \frac{13}{9} \alpha_1(0) h_3 \right) - t \frac{E(t)}{F(t)} + 1 \right], \qquad (4)$$

where $h_i(t) = t/(1 + \beta_i t)$. Therefore the value of A_0 in the IFP limit is irrelevant. Although this is not true for the remaining trilinear couplings A_b, A_τ, etc., the latter A-parameters have a negligible effect in the determination of the Higgs mass, which is the main goal of this paper. The value of $\tan\beta$, evaluated at the scale $Q = M_t$ (where M_t is the physical top-quark mass), is determined by using

$$v_2(M_t) = \frac{m_t(M_t)}{4\pi\sqrt{Y_t(M_t)}}, \qquad (5)$$

---

[3]Of course, these threshold corrections depend on the values of supersymmetric masses and thus on the remaining independent parameters of the model.

and the approximate $\overline{\text{DR}}$ relation [19]

$$v(m_Z) \simeq \left[175.8 + 0.32\ln\left(\frac{m^2 + 4M^2}{m_Z^2}\right)\right]\ \text{GeV}. \tag{6}$$

The distinction between the physical top-quark mass M_t and the running top-quark mass $m_t(M_t)$ should not be ignored. Explicitly, the physical top-quark mass is given by

$$M_t = m_t(M_t)\left[1 + \frac{\Delta m_t}{m_t}\right], \tag{7}$$

where the one-loop correction Δm_t receives two important contributions: the well-known QCD gluon correction[4]

$$\left(\frac{\Delta m_t}{m_t}\right)_{\text{QCD}} = \frac{5g_3^2}{12\pi^2}, \tag{8}$$

and the stop/gluino correction [19,20]

$$\begin{aligned}
\left(\frac{\Delta m_t}{m_t}\right)_{\text{SUSY}} = &-\frac{g_3^2}{12\pi^2}\Bigg\{ B_1(m_t, M_{\tilde{g}}, m_{\tilde{t}_1}) + B_1(m_t, M_{\tilde{g}}, m_{\tilde{t}_2}) \\
&- \sin(2\theta_t)\frac{M_{\tilde{g}}}{m_t}\Big[B_0(m_t, M_{\tilde{g}}, m_{\tilde{t}_1}) - B_0(m_t, M_{\tilde{g}}, m_{\tilde{t}_2})\Big]\Bigg\},
\end{aligned} \tag{9}$$

where θ_t is the stop mixing angle, $m_{\tilde{t}_1} > m_{\tilde{t}_2}$, and

$$B_n(p\,;m_1,m_2) \equiv -\int_0^1 dx\, x^n\, \ln\left[\frac{(1-x)m_1^2 + xm_2^2 - x(1-x)p^2}{m_t^2}\right]. \tag{10}$$

Note that the Standard Model two-loop QCD correction [21] and the electroweak correction [22] are each of order 1% and almost cancel one another. While the one-loop gluon correction [eq. (8)] yields a 6% relative top-quark mass shift, the supersymmetric correction in our scenario is of the same sign and can be as large as the gluon correction for $M \gtrsim 500$ GeV. The stop/gluino correction (which increases with the supersymmetric masses) is a consequence of working in the effective supersymmetric theory without decoupling the supersymmetric particles, as is usually done in the IFP literature when considering the running of Y_t. (In practice, this is the most convenient way to perform the analysis; for an alternative approach, see Ref. [23].) However, the correction given by eq. (9) has never been included in the published analyses of the IFP scenario. This correction has the noteworthy effect of reducing the ratio $m_t(M_t)/M_t$, and consequently lowering the IFP value of $\tan\beta$. As a result, the predicted value for the mass of the light CP-even Higgs boson is significantly reduced, as shown in Section 4.

Let us now turn to the μ-parameter. We noted in Section 1 that μ can be determined (up to a sign) by imposing the condition of electroweak symmetry breaking and fixing the Z mass to its physical value. More precisely, from the minimization of the renormalization-group-improved tree-level Higgs potential, we obtain

$$\mu^2 + \tfrac{1}{2}m_Z^2 = \frac{1}{\tan^2\beta - 1}\left(m_{H_1}^2 - \tan^2\beta\ m_{H_2}^2\right), \tag{11}$$

---

[4]The factor 5 in eq. (8) in the $\overline{\text{DR}}$ scheme should be compared with 4 in the $\overline{\text{MS}}$ scheme [19].

where $m_{H_1}^2, m_{H_2}^2$ are the low-energy values of the soft squared-masses of the H_1, H_2 Higgs fields (subject to the condition $m_{H_1}^2 = m_{H_2}^2 = m^2$ at $Q = M_X$). It is important to note that the result given in eq. (11) is only accurate enough if the tree-level potential is evaluated at a scale where the radiative corrections are minimized. This essentially happens for a scale of order the stop masses [24,25]. From now on we will take that scale, M_S, as the average of the stop squared-mass eigenvalues

$$M_S^2 \equiv \tfrac{1}{2} \left(m_{\tilde{t}_1}^2 + m_{\tilde{t}_2}^2 \right) . \tag{12}$$

Consequently, all the quantities appearing in eq. (11) (including μ and m_Z) are to be taken at $Q = M_S$.[5] From eq. (5), eq. (6) *plus* the renormalization group evolution of H_1, H_2 with their anomalous dimensions, we can determine the value of $\tan\beta$ at any scale using the corresponding RGE for $\tan\beta$:

$$\frac{d\tan\beta}{dt} \simeq \tfrac{3}{2} Y_t \tan\beta . \tag{13}$$

This result can be employed to determine the value of $\tan\beta$ at M_S. The running of $\tan\beta$ has been ignored in the IFP literature and produces significant corrections in the final results.

From eqs. (4)–(6) and eq. (11) it follows that the only relevant independent parameters for predicting the light CP-even Higgs mass m_{h^0} in the IFP scenario are m and M. These can be traded in for M_S and $x \equiv M/m$. Notice that in either case $\mathrm{sign}(\mu)$ may be absorbed, by a redefinition of fields, into the sign of M (or equivalently, the sign of x). Besides the simplicity of this scenario, the fact that all the relevant low-energy quantities can be expressed in terms of M_S and x has important consequences for the prediction of m_{h^0}. In particular, the mass splitting between stops and the effective mixing[6]

$$X_t \equiv A_t + \mu \cot\beta , \tag{14}$$

which play an important role in the computation of m_{h^0} (see Section 3) are no longer independent parameters, but are calculable quantities in terms of M_S and x. Since they cannot be simultaneously "tuned" to the values that maximize m_{h^0}, this produces an effective lowering of the upper bound on m_{h^0}. These issues will be carefully analyzed in the next two sections.

There is yet another source of constraints on the theory, namely the desirable absence of dangerous charge and color breaking (CCB) minima [27,28] or unbounded from below (UFB) directions [28] in the scalar potential. CCB and UFB constraints have been recently analyzed for the IFP scenario [29]. Since all the physics in which we are interested depends on just two parameters, M and m (or equivalently M_S and x), we must focus on the CCB and UFB constraints involving these quantities. This means, in particular, that the CCB constraints involving the trilinear scalar couplings other

---

[5]Even including the one-loop radiative corrections ΔV_1 to the tree-level potential V_0, and using eq. (11) accordingly modified, is not in general a precise procedure since $V_0 + \Delta V_1$ at $Q = m_Z$ still yields inaccurate results if $M_S^2 \gg m_Z^2$, as it is normally the case [25] (see the comments at the end of the appendix).

[6]The convention for the sign of μ in eq. (14) is opposite to the one employed in Ref. [26].

than the top one, *i.e.* A_u, A_d, A_s, etc., have no relevance to us since their low-energy values may be tuned at will by varying the initial high-energy parameter A_0. This is not the case for the low-energy top trilinear scalar coupling A_t, which in our scenario is driven to an infrared fixed point given by eq. (4) [more generally, by eq. (32)], namely $A_t \simeq -1.2M$. This value, however, is well inside the region allowed by the CCB bounds [29]. On the other hand, UFB bounds strongly restrict the $x \equiv M/m$ parameter [29] in the IFP scenario, namely the absence of UFB directions requires $|x| \leq 1$. In any case, the results presented in Section 4 imply that for $x > 1$ the value of m_{h^0} hardly changes as a function of x (*i.e.* it already reaches its large-x asymptotic limit at $x = 1$). Thus, in practice the CCB and UFB constraints do not restrict the bounds on m_{h^0} in the IFP scenario.

3 The MSSM Higgs mass

The Higgs sector of the MSSM consists of five physical states: two neutral CP-even scalars h^0 and H^0 (with $m_{h^0} \leq m_{H^0}$), one neutral CP-odd scalar A^0, and a charged Higgs pair $H^\pm$. The quadratic terms of the Higgs potential consists of two diagonal squared-mass terms: $m_i^2 \equiv m_{H_i}^2 + |\mu|^2$, and one off-diagonal squared-mass term: m_{12}^2. When the minimum condition is imposed, the diagonal squared-mass terms are traded in for the vacuum expectation values v_1 and v_2. Thus, the tree-level Higgs sector depends on only two new parameters: $\tan\beta$ and m_{12}^2. It is convenient to replace m_{12}^2 with the physical parameter m_{A^0}. Then, all other Higgs masses and couplings can be expressed at tree level in terms of $\tan\beta$ and m_{A^0}.

The prediction for the mass of the lightest CP-even neutral Higgs boson is of particular interest to the LEP Higgs search, since this Higgs scalar would be discovered first if it lies within the reach of the LEP-2 collider. In particular, the MSSM predicts that at tree level, $m_{h^0} \leq m_Z |\cos 2\beta| \leq m_Z$. When radiative corrections are included, the light Higgs mass upper bound may be significantly increased above the tree level prediction. This has profound effects on the LEP Higgs search. LEP-2 running at its maximum energy ($\sqrt{s} \simeq 200$ GeV) and luminosity is expected to be sensitive to Higgs masses up to about 105 GeV [30]. Thus, the possibility of large radiative corrections to m_{h^0} implies that LEP cannot be sensitive to the full MSSM Higgs sector parameter space.

The mass of h^0 can be calculated in terms of the two parameters of the Higgs sector mentioned above (m_{A^0} and $\tan\beta$) and other MSSM soft-supersymmetry-breaking parameters that affect the Higgs mass through virtual loops [31,32,33,34,35,36,37,38,39,40]. The largest contribution to the one-loop radiative corrections is enhanced by a factor of m_t^4 and grows logarithmically with the stop mass. Thus, higher-order radiative corrections can be non-negligible for large stop masses, in which case the large logarithms must be resummed using renormalization group techniques [35,36,37,38,39,40].

For our numerical work, we will follow the simple analytic procedure for accurately approximating m_{h^0} described in Ref. [40], where further details can be found. Similar results are obtained by using the alternative approximation of Refs. [38,39]. These analytic formulae incorporate both the leading one-loop and two-loop effects and the RG

improvement. Also included are the leading effects at one loop of the supersymmetric thresholds (the most important effects of this type are squark mixing effects in the third generation).

In the limit $m_{A^0} \gg m_Z$, which holds in the IFP scenario, only h^0 remains light (with couplings nearly identical to those of the Standard Model Higgs boson), and its squared-mass including RG improvement is given by a formula of the form[7] [40]

$$m_{h^0}^2 \simeq (m_{h^0}^2)_{\text{1LL}} \left[m_t(\mu_t) \right] + (\Delta m_{h^0}^2)_{\text{mix}} \left[m_t(\mu_{\tilde{t}}) \right] , \qquad (15)$$

where

$$\mu_t \equiv \sqrt{m_t M_{\text{S}}} , \qquad \mu_{\tilde{t}} \equiv M_S . \qquad (16)$$

In particular, the numerically integrated RG-improved CP-even Higgs mass is well approximated by replacing all occurrences of m_t in $(m_{h^0}^2)_{\text{1LL}}$ and $(\Delta m_{h^0}^2)_{\text{mix}}$ by the corresponding running masses evaluated at the judicious choice of scales indicated above.

The first term in eq. (15) is the one-loop leading logarithmic contribution to the squared mass, given by

$$(m_{h^0}^2)_{\text{1LL}} \simeq m_Z^2 \cos^2 2\beta + \frac{g^2 N_c m_t^4(\mu_t)}{8\pi^2 m_W^2} \ln \left(\frac{m_{\tilde{t}_1} m_{\tilde{t}_2}}{m_t^2} \right) , \qquad (17)$$

where $\tan \beta$ is evaluated at m_Z and $N_c = 3$. Subdominant terms not written in eq. (17) can also be important for a precise determination of m_{h^0}. They can be found in Ref. [40] and were included in our numerical analysis. The second term in eq. (15) adds the important effects of stop mixing; it takes the form (again we display here only the dominant terms)

$$(\Delta m_{h^0}^2)_{\text{mix}} \simeq \frac{g^2 N_c}{16\pi^2 m_W^2} m_t^4(\mu_{\tilde{t}}) \left\{ X_t^2 \left[2h(m_{\tilde{t}_1}^2, m_{\tilde{t}_2}^2) + X_t^2 g(m_{\tilde{t}_1}^2, m_{\tilde{t}_2}^2) \right] \right\}, \qquad (18)$$

where X_t is given by eq. (14), and

$$
\begin{aligned}
h(a, b) &= \frac{1}{a - b} \ln \frac{a}{b} , \\
g(a, b) &= \frac{1}{(a - b)^2} \left(2 - \frac{a + b}{a - b} \ln \frac{a}{b} \right) .
\end{aligned}
\qquad (19)
$$

Using these results, the full (numerically integrated) RG-improved value of m_{h^0} is reproduced to within an accuracy of about 2 GeV (assuming that supersymmetric particle masses lie below 2 TeV).

For $|m_{\tilde{t}_1}^2 - m_{\tilde{t}_2}^2| \ll M_S^2$, we may approximate $g(a, a) \simeq -1/6a^2$ and $h(a, a) \simeq 1/a$. Then eq. (18) simplifies and takes the form

$$(\Delta m_{h^0}^2)_{\text{mix}} = \frac{g^2 N_c}{16\pi^2 m_W^2} m_t^4 \left\{ \frac{2X_t^2}{M_S^2} \left(1 - \frac{X_t^2}{12M_S^2} \right) \right\} . \qquad (20)$$

---

[7]Corrections associated with sbottom virtual loops are small if $\tan \beta$ is small, and so they are not shown explicitly in eq. (15), although they were included in our numerical analysis.

From eq. (20) it is easy to see that the maximal value of $(\Delta m_{h^0}^2)_{\text{mix}}$, and thus m_{h^0}, is achieved for $|X_t| = \sqrt{6}M_{\text{S}}$, which is sometimes called "maximal mixing". For this value of $|X_t|$, the quantity in curly brackets in eq. (20) is equal to 6. For larger values of $|X_t|$ this correction decreases, eventually turning negative. In the IFP scenario the approximation of nearly degenerate stops is not always applicable (particularly for small values of $|x|$, as shown in fig. 1), and one must include the stop mixing corrections in its full form [eq. (18)]. In the latter case, $(\Delta m_{h^0}^2)_{\text{mix}}$ does not follow the simple behaviour discussed for the approximately mass-degenerate case; for example, values larger than 6 for the term in curly brackets in eq. (18) can result.
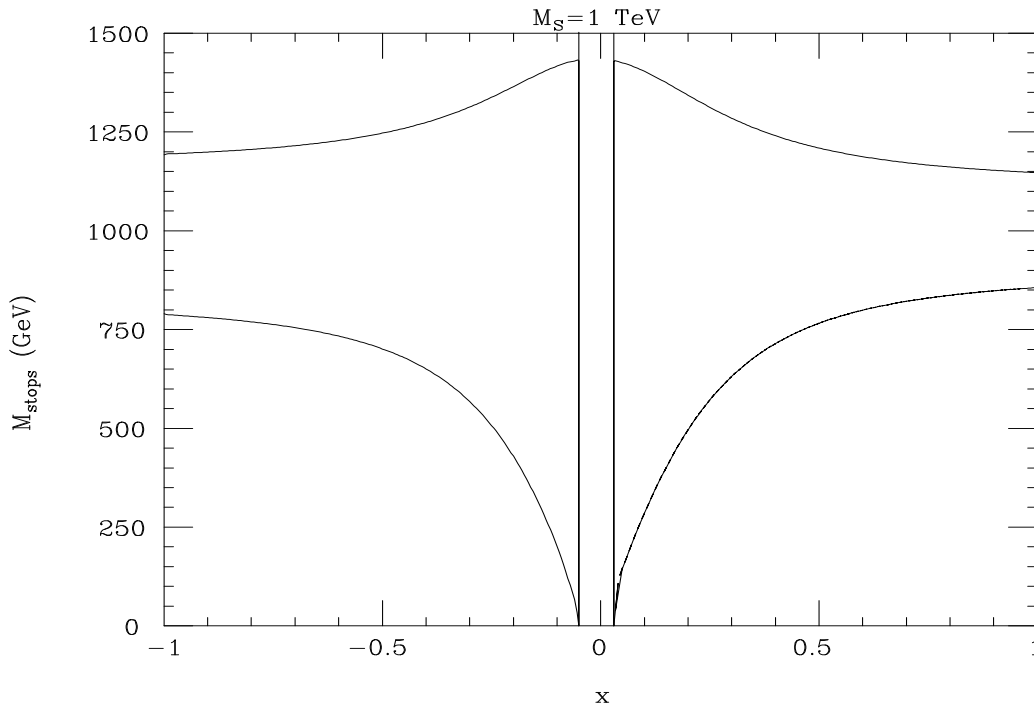

Figure 1: Stop-mass eigenvalues $m_{\tilde{t}_1}$ (upper curves), $m_{\tilde{t}_2}$ (lower curves), as a function of $x = M/m$ in the IFP scenario for $M_S = 1$ TeV and $M_t = 175$ GeV. The indicated area around $x = 0$ has one very light stop (or a negative value of $m_{\tilde{t}_2}^2$) and is thus excluded experimentally.

As an example, one finds the following mass bounds for h^0, assuming $M_t = 175$ GeV and $M_S \lesssim 1$ TeV: $m_{h^0} \lesssim 112$ GeV if stop mixing is negligible, while $m_{h^0} \lesssim 125$ GeV if stop mixing is "maximal". In both cases the upper bound corresponds to large $\tan\beta$. When the IFP scenario is imposed, the parameter restrictions examined in Section 2 (*e.g.* both $\tan\beta$ and A_t are driven to fixed-point values) imply that the Higgs mass upper limits quoted above are not saturated. Consequently the predicted value of m_{h^0} decreases substantially. In Section 4, we shall explore in detail the predictions for m_{h^0} in the IFP scenario as a function of the remaining free parameters.

4 Results

For the sake of definiteness and to facilitate the comparison with previous results in the literature, we first present detailed results for $M_S = 1$ TeV. Subsequently, we will allow M_S to vary. It is then illustrative to start by showing the dependence of several relevant quantities as a function of the only remaining parameter, $x \equiv M/m$. In all the cases we will vary x over the range $[-1, 1]$, since for $|x| \geq 1$ all the relevant quantities enter an asymptotic regime, as will be apparent from the figures. In addition, as explained at the end of Section 2, the values $|x| \gtrsim 1$ are in conflict with CCB and UFB bounds.

In fig. 1 we plot the two stop mass eigenvalues $m_{\tilde{t}_1}, m_{\tilde{t}_2}$ as a function of x. We note that for $-0.07 \lesssim x \lesssim 0.03$ the mass of the lightest stop is lower than the present experimental bounds [41]. Thus, this region is excluded, as indicated in all figures shown in this section. We also observe that eq. (20) is no longer a good approximation for $(\Delta m_{h^0}^2)_{\mathrm{mix}}$ when $|x| \lesssim 0.4$, and one must use eq. (18), as noted at the end of Section 3.
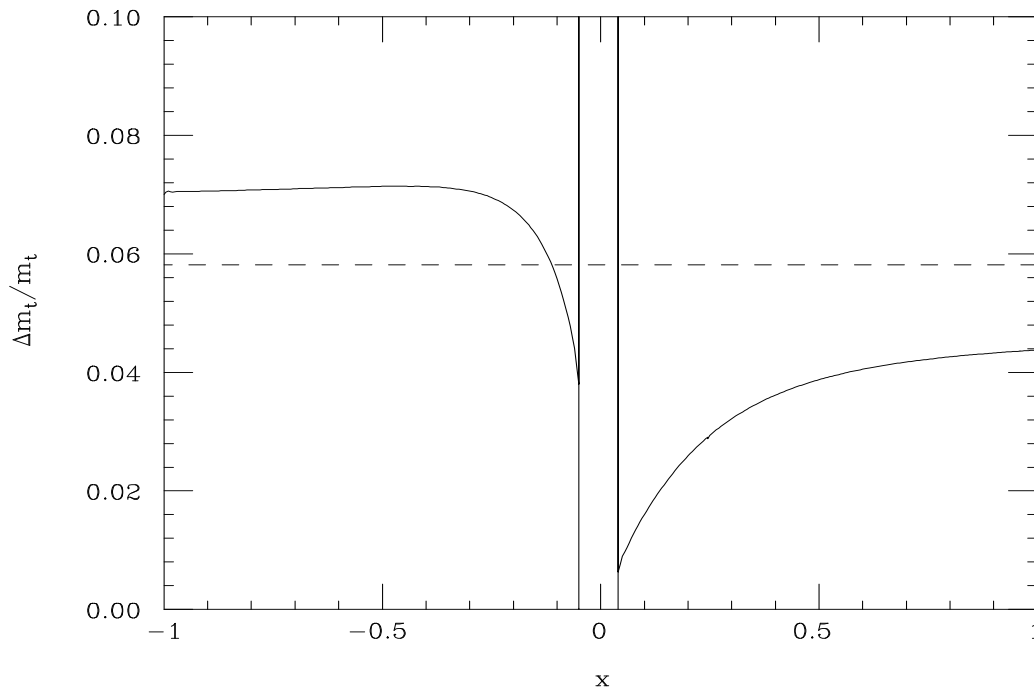

Figure 2: Stop/gluino threshold contribution [eq. (9)] to the relationship between the physical (pole) top-quark mass M_t and the $\overline{\mathrm{DR}}$ running mass $m_t \equiv m_t(M_t)$, as a function of $x \equiv M/m$ in the IFP scenario with $M_S = 1$ TeV and $M_t = 175$ GeV (solid line). For comparison, the gluon contribution [eq. (8)] is also exhibited (dashed line).

Figure 2 shows the supersymmetric correction (due to stop/gluino loops) to the top-quark mass $(\Delta m_t/m_t)_{\mathrm{SUSY}}$ as a function of x. Note that this correction is in general quite important. For comparison, we have also plotted the usual QCD correction, $(\Delta m_t/m_t)_{\mathrm{QCD}}$ (constant dashed line). Although the supersymmetric correction does not always have a definite sign in general models (as noted in Ref. [12]), this correction

9

is always of the same sign as the QCD correction in the IFP scenario considered in this paper. This feature is a result of the constraints imposed on the stop and gluino masses. Moreover, the larger the positive value of Δm_t, the lower the value of $\tan \beta$. This can be seen from the dashed line in fig. 3, which shows the behaviour of $\tan \beta$ as a function of x.
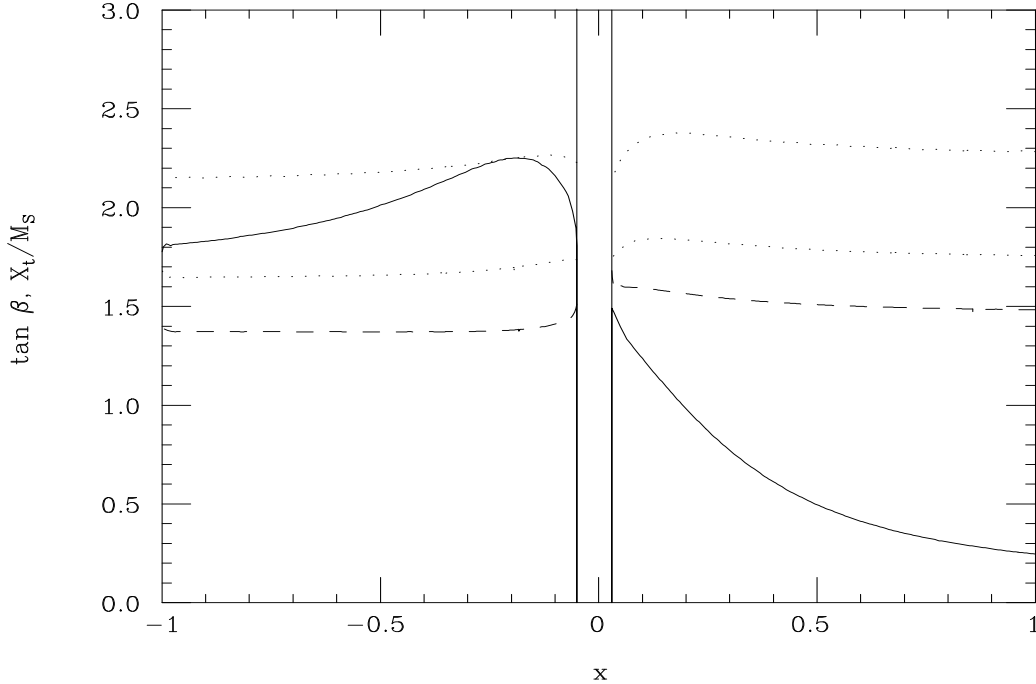

Figure 3: Predicted value of the stop mixing parameter X_t/M_S (solid line) and $\tan \beta$ (dashed line) in the IFP scenario as a function of $x \equiv M/m$ with $M_S = 1$ TeV and $M_t = 175$ GeV. Both parameters are essential in the determination of m_{h^0}. The dotted lines indicate the value of $\tan \beta$ if one moves away from the IFP limit of $Y_t = Y_f$ [see eq. (3)]; the upper [lower] dotted line corresponds to $Y_t/Y_f = 0.8$ [0.9].

Figure 3 also shows the value of X_t/M_S as a function of x. Recall that both $\tan \beta$ and X_t/M_S have a crucial impact on m_{h^0}. In particular (assuming that $\tan \beta \geq 1$ and $|X_t/M_S| \leq \sqrt{6}$, which is always true in the IFP scenario considered here), m_{h^0} is an increasing function of both $\tan \beta$ and $|X_t/M_S|$. However, as seen from fig. 3, $\tan \beta$ and $|X_t/M_S|$ do not attain their maximum values at the same value of x, which leads to an effective lowering of the maximum possible value of m_{h^0}. Moreover, X_t/M_S never reaches the "maximal value" of $|X_t/M_S| = \sqrt{6}$. This again limits the maximal value of m_{h^0} to lie below its MSSM upper bound.

The behaviour of X_t/M_S shown in fig. 3 can be understood by using eqs. (14) and (12) plus the expressions for μ, A_t and the third-generation scalar squared-masses given in Section 2 and the appendix. In the limit where $M_S \gg m_t$, we obtain

$$\frac{X_t}{M_S} \simeq \frac{-1.2 \, x + \cot \beta (\tan^2 \beta - 1)^{-1/2} \left[(1 + 0.5 \tan^2 \beta) + (0.5 + 2 \tan^2 \beta) \, x^2 \right]^{1/2}}{(0.25 + 2.75 \, x^2)^{1/2}} \, . \quad (21)$$

10

For a typical value of $\tan\beta$ (*e.g.* $\tan\beta \sim 1.5$ according to fig. 3), eq. (21) reaches a maximum at $x \sim -0.2$ and lies below the "maximal value" $|X_t/M_S| = \sqrt{6}$.
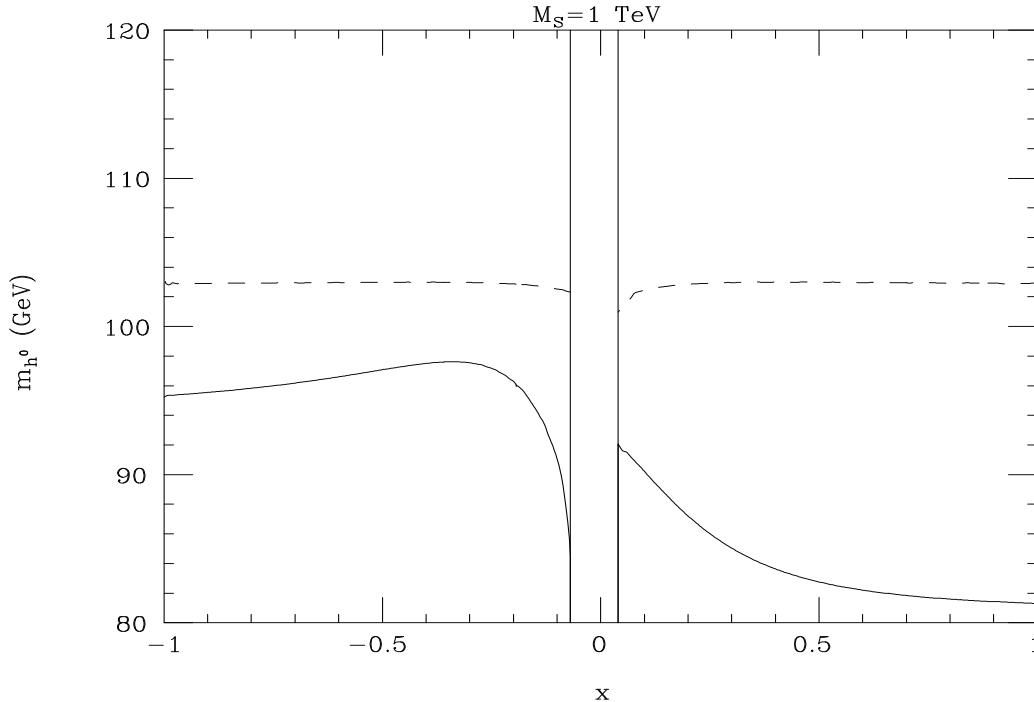

Figure 4: Different approximations to the lightest CP-even Higgs mass as a function of $x \equiv M/m$ for the IFP scenario with $M_S = 1$ TeV and $M_t = 175$ GeV. The result of the calculation of this paper is given by the solid curve. If one omits the stop/gluino loop corrections to $M_t/m_t(M_t)$ and assumes maximal stop mixing, one obtains the dashed curved.

In fig. 4, the solid curve depicts the results for m_{h^0} in the IFP scenario considered in this paper, with $M_S = 1$ TeV and $M_t = 175$ GeV. Note that the absolute upper bound on m_{h^0} corresponds to $x \sim -0.3$, although for $x \lesssim -0.1$, the variation of m_{h^0} with x is small. Numerically the bound on m_{h^0} reads $m_{h^0} \leq 97$ GeV, with an estimated error of ± 2 GeV (this error is based on the results of Ref. [40]). In order to illustrate the impact of the new effects that we have incorporated into the calculation of m_{h^0}, we exhibit the dashed curve in fig. 4. This latter curve results from a calculation in which the stop/gluino corrections to the physical (pole) top-quark mass M_t, in terms of the $\overline{\text{DR}}$ running mass $m_t(M_t)$, are omitted [*i.e.* taking $(\Delta m_t/m_t)_{\text{SUSY}} = 0$], and the stop mixing parameter is set at its "maximal" value, $|X_t/M_S| = \sqrt{6}$. This procedure has been used in some works [37,38,39] to deduce an absolute upper bound on m_{h^0} in the IFP scenario. In addition, following Refs. [37,38], eq. (20) was used to obtain the dashed curve for all values of x, although we know (see the discussion near the end of Section 3) that the underlying assumption of nearly degenerate stops is not appropriate for $|x| \lesssim 0.3$. (The effects of non-degenerate stops were taken into account in Ref. [39].) As anticipated, the dashed curve of fig. 4 significantly overestimates the m_{h^0} bound over the full x range. Quantitatively, the overestimate is ~ 7 GeV for $x < 0$ and ~ 20 GeV for $x > 0$.

We conclude that previous results for m_{h^0} in the IFP scenario obtained in the literature had neglected a number of significant effects, which lead to a substantial reduction in the prediction of the upper bound for m_{h^0} as a function of the minimal SUGRA parameters. The Higgs mass upper bounds obtained previously are therefore too conservative. The more refined bound of $m_{h^0} \lesssim 100$ GeV, obtained in this paper, is significant in that it lies within the reach of the LEP-2 Higgs search once the maximum LEP-2 energy and luminosity is achieved.
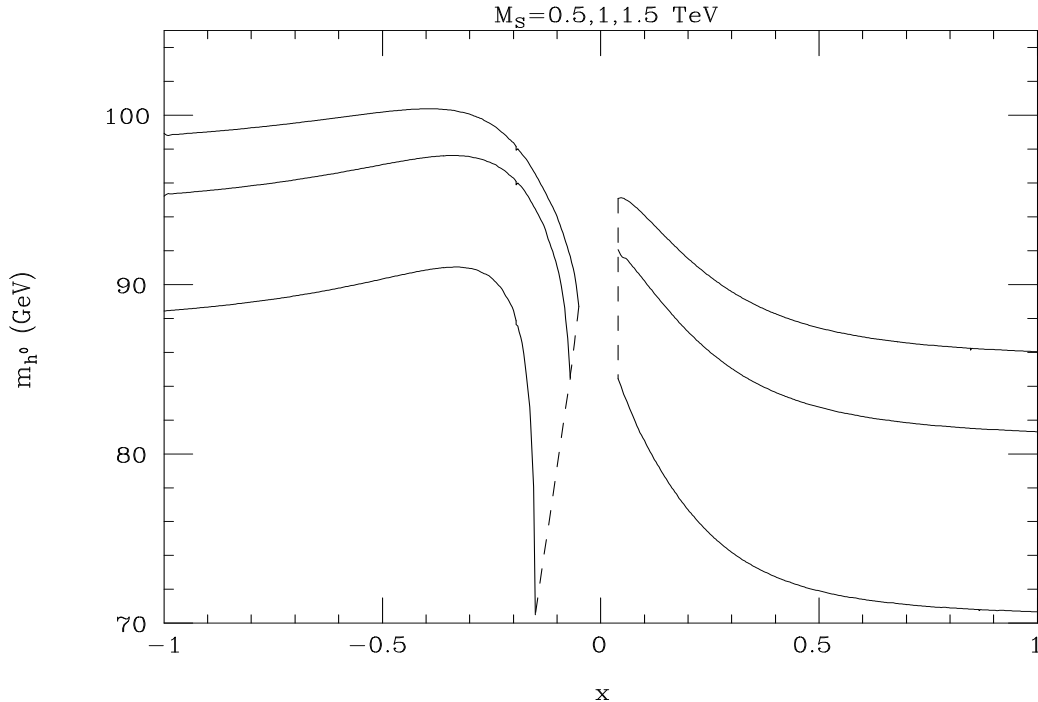

Figure 5: Lightest CP-even Higgs mass as a function of $x \equiv M/m$ in the IFP scenario for $M_t = 175$ GeV and different values of M_S. The curves shown correspond to $M_S = 0.5$ TeV (lower curve), $M_S = 1$ TeV (middle curve) and 1.5 TeV (upper curve). For small x, the curves end at the dashed lines where the stop mass lies below its experimental bound.

We next consider the effect of varying the other relevant model parameters. Figure 5 shows the value of m_{h^0} as a function of x for different values of M_S; curves for $M_S = 0.5$ TeV, 1 TeV, and 1.5 TeV are shown. As expected, the predicted value of m_{h^0} increases logarithmically with M_S. Figure 5 clearly shows a marked asymmetry in the predicted value of m_{h^0} under a change of sign of x. For $x > 0$, the stop mixing contribution to m_{h^0} is less important since a destructive cancellation takes place between A_t and μ in X_t (see fig. 3). As a result, m_{h^0} is typically less than 90 GeV, which is almost excluded by the current LEP-2 limits on m_{h^0} [42]. For $x < 0$, A_t and μ have the same sign, thereby enhancing X_t. The corresponding value of m_{h^0} is larger in this case, although for $M_S \leq 1.5$ TeV, we still predict $m_{h^0} \lesssim 100$ GeV. Larger values for M_S are less plausible, assuming that electroweak symmetry breaking is a natural consequence of low-energy supersymmetry.
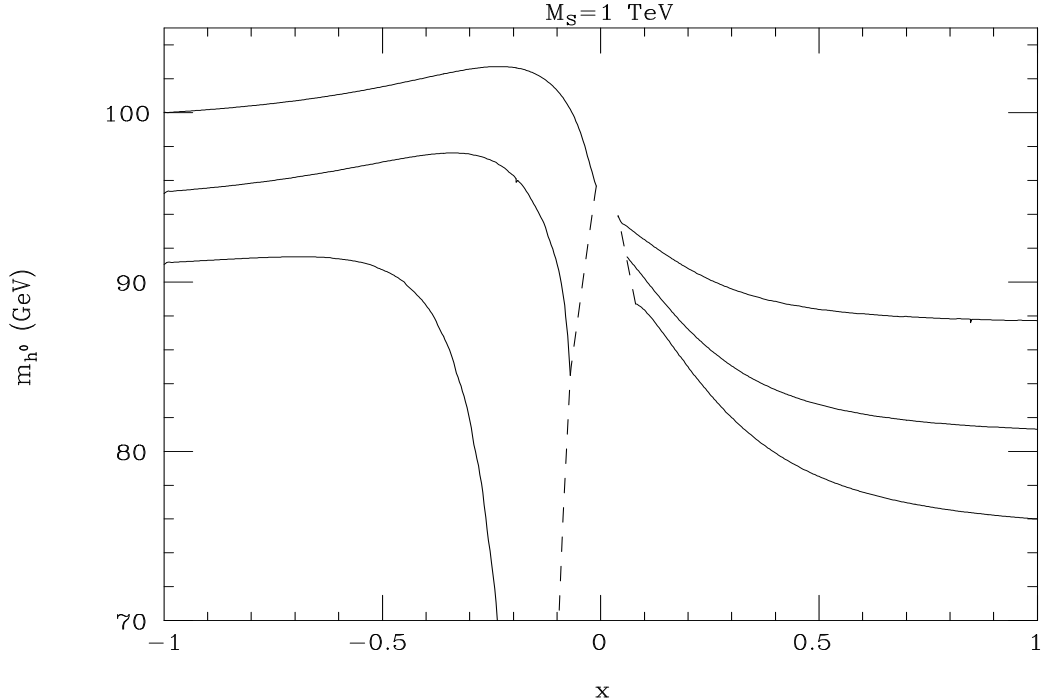
Figure 6: Lightest CP-even Higgs mass as a function of $x \equiv M/m$ in the IFP scenario for $M_S = 1$ TeV and different values of M_t. The curves shown correspond to $M_t = 170$ GeV (lower curve), $M_t = 175$ GeV (middle curve) and 180 GeV (upper curve).

The predicted value of m_{h^0} is quite sensitive to the value of the top mass, due to the m_t^4 behavior exhibited in eq. (17). Taking into account the experimental error of about 5 GeV in the measured top quark mass, we exhibit in fig. 6 the predicted value of m_{h^0} as a function of x for $M_S = 1$ TeV and three choices of top quark mass. For the maximal value of $M_t = 180$ GeV, we see that the predicted upper bound of m_{h^0} is increased by about 5 GeV, compared to the previous results shown (for the central value of $M_t = 175$ GeV). We also note that for $M_t = 180$ GeV, the x dependence is somewhat less pronounced, with the predicted value of m_{h^0} above 88 GeV over the entire allowed range of x. If we impose $M_S \leq 1.5$ TeV, we conclude that the upper bound of the light CP-even Higgs mass in the IFP scenario is about 95–105 GeV (for $M_t = 175 \pm 5$ GeV), although the upper bound is not saturated over a significant region of the minimal SUGRA parameter space.

5   Conclusions

The quasi-infrared fixed point model is very attractive, since a number of quite general and well-motivated initial conditions lead to a highly predictive low-energy scenario. More precisely, working within the SUGRA framework (with the assumption of universality of scalar and gaugino soft-supersymmetry-breaking masses), the only two independent parameters for low-energy physics are the common (high-energy) scalar

(m) and gaugino (M) masses. We have studied in this framework the value of the light CP-even Higgs mass, m_{h^0}, which is a particularly relevant physical quantity since it turns out to be greatly constrained. We have taken into account some important effects that had not been previously considered. The most notable of these is the supersymmetric correction to the relation between the running and the physical top-quark masses, which lowers the value of $\tan\beta$ and thus that of m_{h^0}. Other effects arise from the precise determination of the stop mixing parameter X_t (which plays a major role in the computation of m_{h^0}), as well as the observation that $\tan\beta$ and X_t never conspire to raise m_{h^0} to its maximum possible value. In addition we have computed m_{h^0} using the most refined available method, including subdominant contributions and corrections from stop non-degeneracy. This substantially reduces the theoretical uncertainty of our results with respect to previous calculations in the literature.

Our predictions for m_{h^0} are significantly lower than previous evaluations, as illustrated in fig. 4. Figure 5 displays our calculation of m_{h^0} and exhibits its dependence on $x \simeq M/m$ for different values of $M_S^2 \equiv \frac{1}{2}\left(m_{\tilde{t}_1}^2 + m_{\tilde{t}_2}^2\right)$. For $M_S \leq 1$ TeV and $M_t = 175$ GeV we find $m_{h^0} \leq 97 \pm 2$ GeV; the upper bound increases slightly for larger values of M_S and M_t. For sensible parameter choices, we conclude that $m_{h^0} \lesssim 105$ GeV in the IFP scenario based on the constrained MSSM with universal scalar and gaugino mass parameters (as in minimal SUGRA and some superstring models), and that the most plausible m_{h^0} values may be substantially smaller. These values of m_{h^0} are within the reach of the LEP-2 Higgs search.

If LEP-2 fails to discover the h^0, then one will be able to rule out the IFP scenario in the context of SUGRA models with universal boundary conditions. Of course, this will not rule out all possible SUGRA models (or more general versions of the MSSM), where the upper bound $m_{h^0} \lesssim 125$ GeV quoted at the end of Section 3 can still be realized. Nevertheless, it is worth emphasizing that the IFP scenario does not correspond merely to a single point of the supersymmetric parameter space. As noted in Section 1, as long as $Y_t(0) \gtrsim 0.01$, the low-energy values of A_t and $\tan\beta$ converge quite closely to their IFP limits (and independently of the value of the high-energy parameter A_0). Thus, the IFP prediction of the Higgs mass bound presented in this paper corresponds to a non-negligible region of the space of supersymmetric parameters at the high-energy scale.

Finally, it is interesting to note that the bound on m_{h^0} obtained in this paper is quite robust. The effect of a small deviation from the IFP limit leads only to a modest increase in the mass bound of the light CP-even Higgs boson. For example, suppose we take the value of Y_t to lie somewhat below its fixed point value Y_f, but still close enough such that the dependence of A_t on its high-energy value A_0 is negligible. Then, we find that $\tan\beta$ increases from its predicted IFP value, while X_t/M_S decreases throughout the x range of interest. As a result of these two opposing effects, we find that the upper bound of m_{h^0} barely shifts (although in contrast with the results of figs. 4–6, the bound on m_{h^0} as a function of x is much flatter). As one takes Y_t further away from the IFP limit, the dependence of X_t on A_0 can no longer be neglected. One can now attain maximal mixing for reasonable choices of A_0. Since $\tan\beta$ is increased from its IFP value, the upper bound on m_{h^0} also increases. To illustrate these considerations, we computed the light CP-even Higgs mass for $M_S = 1$ TeV and $m_t = 175$ GeV as Y_t

is reduced below Y_f. Using the results for $\tan\beta$ shown by the dotted curves in fig. 3, we find that the upper bound on m_{h^0} (which was 97 GeV in the IFP limit) increases to about 103 GeV [110 GeV], for $Y_t/Y_f = 0.9$ [0.8]. Note that away from the IFP limit, the upper bound on m_{h^0} is nearly independent of the value of x (since the dependence on x in this case enters mainly through $\tan\beta$). Thus, if h^0 is not discovered at LEP-2, then one must be somewhat far from the IFP limit examined in this paper. Given that LEP-2 expects to reach its maximal energy and luminosity during the next two years, it is safe to say that the decisive test for the IFP scenario will soon be at hand.

Acknowledgements

Appendix

Starting with universal scalar (m) and gaugino (M) soft masses at the unification scale $M_X = [1.2 - 0.32t_s + 0.17t_s^2] \times 10^{16}$ GeV, [8] the soft masses at the supersymmetric scale [of order M_S, with $t_s \equiv \ln(M_S/1\text{ TeV})$] are:

$$m_{H_1}^2 = m^2 + 0.5M^2 \tag{22}$$

$$m_{H_2}^2 = m^2 + 0.5M^2 + \Delta m^2 \tag{23}$$

$$m_{L_i}^2 = m^2 + 0.5M^2 \tag{24}$$

$$m_{E_i}^2 = m^2 + 0.1M^2 \tag{25}$$

$$m_{Q_i}^2 = m^2 + [4.2 - 0.69t_s + 0.46t_s^2]M^2 + \tfrac{1}{3}\delta_{i3}\Delta m^2 \tag{26}$$

$$m_{U_i}^2 = m^2 + [3.8 - 0.69t_s + 0.46t_s^2]M^2 + \tfrac{2}{3}\delta_{i3}\Delta m^2 \tag{27}$$

$$m_{D_i}^2 = m^2 + [3.7 - 0.69t_s + 0.46t_s^2]M^2 \,, \tag{28}$$

where the labels $H_{1,2}$ are used for the soft masses of the Higgs doublets, L for the slepton doublets, E for the singlet sleptons, Q for the doublet squarks and U, D for up and down singlet squarks (i is a family index), and

$$\begin{aligned}
\Delta m^2 = \quad & -\tfrac{3}{2}m^2\frac{Y_t}{Y_f} + \left([1.6 - 0.19t_s + 0.1t_s^2]A_0 M - \tfrac{1}{2}A_0^2\right)\frac{Y_t}{Y_f}\left(1 - \frac{Y_t}{Y_f}\right) \\
& + M^2\frac{Y_t}{Y_f}\left([1.3 - 0.34t_s + 0.1t_s^2]\frac{Y_t}{Y_f} - [3.8 - 0.69t_s + 0.6t_s^2]\right), \quad (29)
\end{aligned}$$

---

[8]This result exhibits the dependence of M_X on the supersymmetric scale M_S. The numerical coefficients of the prefactor are based on a fit to results obtained from a numerical integration of the two-loop RGEs, with $\alpha(M_X) = 0.039$.

where, following ref. [7], we have expressed our results in terms of the ratio Y_t/Y_f.

In addition[9],

$$\mu^2 = 1.8\mu_0^2 \left(1 - \frac{Y_t}{Y_f}\right)^{1/2} , \tag{30}$$

$$B = B_0 - \tfrac{1}{2}A_0\frac{Y_t}{Y_f} - M \left(0.5 - [0.8 - 0.1t_s + 0.045t_s^2]\frac{Y_t}{Y_f}\right) , \tag{31}$$

$$A_t = A_0 \left(1 - \frac{Y_t}{Y_f}\right) - M \left([2.8 - 0.31t_s + 0.3t_s^2] - [1.6 - 0.2t_s + 0.09t_s^2]\frac{Y_t}{Y_f}\right) . \tag{32}$$

In the above, the fitting of the numerical coefficients is accurate in the range $500\,\text{GeV} \leq M_S \leq 1500\,\text{GeV}$. Note that the values of the above parameters at M_S (particularly those whose running is affected by α_s, such as the squark squared-mass parameters and A_t) are substantially different from the corresponding values at m_Z (see Ref. [7]).

References

[1] S. Dimopoulos and H. Georgi, *Nucl. Phys.* **B193** (1981) 150; H. Georgi, *Phys. Lett.* **169B** (1986) 231; L.J. Hall, V.A. Kostelecky and S. Raby *Nucl. Phys.* **B267** (1986) 415.

[2] H.P. Nilles, *Phys. Rep.* **110** (1984) 1.

[3] B. de Carlos, J.A. Casas and C. Muñoz, *Phys. Lett.* **B299** (1993) 234; V. Kaplunovsky and J. Louis, *Phys. Lett.* **B306** (1993) 269; A. Brignole, L.E. Ibáñez and C. Muñoz, *Nucl. Phys.* **B422** (1994) 125; J. A. Casas, *Phys. Lett.* **B384** (1996) 103.

[4] C.T. Hill, *Phys. Rev.* **D24** (1981) 691; C.T. Hill, C.N. Leung and S. Rao, *Nucl. Phys.* **B262** (1985) 517.

[5] L. Ibáñez and C. López, *Nucl. Phys.* **B233** (1984) 511.

[6] V. Barger, M. S. Berger, P. Ohmann and R. J. N. Phillips, *Phys. Lett.* **B314** (1993) 351.

[7] M. Carena, M. Olechowski, S. Pokorski and C.E.M. Wagner, *Nucl. Phys.* **B419** (1994) 213.

[8] M. Carena and C.E.M. Wagner, *Nucl. Phys.* **B452** (1995) 45.

[9] M. Lanzagorta and G.G. Ross, *Phys. Lett.* **B349** (1995) 319.

---

[9]It may seem that eq. (30) is in conflict with eq. (11) in the quasi-infrared fixed point limit. Strictly speaking, we never reach this limit, so Y_t differs from Y_f by a small amount. Thus, in practice the low-energy value of μ is first obtained from eq. (11), and then μ_0 is deduced from eq. (30). Clearly, $\mu_0 \gg \mu$ for $Y_t \simeq Y_f$, which is equivalent to an unnatural fine-tuning in the electroweak symmetry breaking condition. Nevertheless, one can still be in the domain of the IFP solution without significantly violating the naturalness requirements.

[10] B. Schrempp and M. Wimmer, *Prog. Part. Nucl. Phys.* **37** (1996) 1.

[11] P. Langacker and N. Polonsky, *Phys. Rev.* **D50** (1994) 2199.

[12] J. Feng, N. Polonsky and S. Thomas, *Phys. Lett.* **B370** (1996) 95; N. Polonsky, *Phys. Rev.* **D54** (1996) 4537.

[13] P. Chankowski and S. Pokorski, in *Perspectives on Higgs Physics II*, edited by G.L. Kane (World Scientific, Singapore, 1997) pp. 181–207.

[14] B. Brahmachari, *Mod. Phys. Lett.* **A12** (1997) 1969.

[15] S. Abel and B. Allanach, *Phys. Lett.* **B415** (1997) 371.

[16] B. Pendleton and G.G. Ross, *Phys. Lett.* **98B** (1981) 291.

[17] A.E. Nelson and L. Randall, *Phys. Lett.* **B316** (1993) 516; R. Rattazzi and U. Sarid, *Phys. Rev.* **D53** (1996) 1553.

[18] P.M. Ferreira, I. Jack and D.R.T. Jones, *Phys. Lett.* **B392** (1997) 376.

[19] D.M. Pierce, hep-ph/9407202; J.A. Bagger, K. Matchev and D.M. Pierce, *Phys. Lett.* **B348** (1995) 443; J.A. Bagger, K. Matchev, D.M. Pierce and R. Zhang, *Nucl. Phys.* **B491** (1997) 3.

[20] B.D. Wright, hep-ph/9404217; A. Donini, *Nucl. Phys.* **B467** (1996) 3.

[21] N. Gray, D.J. Broadhurst, W. Grafe and K. Schilcher, *Z. Phys.* **C48** (1990) 673.

[22] R. Hempfling and B.A. Kniehl, *Phys. Rev.* **D51** (1995) 1386.

[23] T. Kobayashi and Y. Yamagishi, *Phys. Lett.* **B381** (1996) 169.

[24] G. Gamberini, G. Ridolfi and F. Zwirner, *Nucl. Phys.* **B331** (1990) 331; R. Arnowitt and P. Nath, *Phys. Rev.* **D46** (1992) 3981.

[25] B. de Carlos and J.A. Casas, *Phys. Lett.* **B309** (1993) 320.

[26] H.E. Haber, in *Supersymmetry Part I (Theory)*, in the Particle Data Group mini-review, 1997 off-year partial update for the 1998 edition (URL: http://pdg.lbl.gov/)

[27] J.M. Frère, D.R.T. Jones and S. Raby, *Nucl. Phys.* **B222** (1983) 11; L. Alvarez-Gaumé, J. Polchinski and M. Wise, *Nucl. Phys.* **B221** (1983) 495; J.P. Derendinger and C.A. Savoy, *Nucl. Phys.* **B237** (1984) 307; C. Kounnas, A.B. Lahanas, D.V. Nanopoulos and M. Quirós, *Nucl. Phys.* **B236** (1984) 438; J.F. Gunion, H.E. Haber and M. Sher, *Nucl. Phys.* **B306** (1988) 1; A. Kusenko, P. Langacker and G. Segré, *Phys. Rev.* **D54** (1996) 5824.

[28] J.A. Casas, C. Muñoz and A. Lleyda, *Nucl. Phys.* **B471** (1996) 3.

[29] J.A. Casas, A. Lleyda and C. Muñoz, *Phys. Lett.* **B389** (1996) 305.

[30] M. Carena, P.M. Zerwas (conveners), in *Physics at LEP2*, eds. G. Altarelli, T. Sjöstrand and F. Zwirner (CERN Report 96-01, Geneva, 1996) Volume 1, pp. 351–462.

[31] H.E. Haber and R. Hempfling, *Phys. Rev. Lett.* **66** (1991) 1815; Y. Okada, M. Yamaguchi and T. Yanagida, *Prog. Theor. Phys.* **85** (1991) 1 ; J. Ellis, G. Ridolfi and F. Zwirner, *Phys. Lett.* **B257** (1991) 83 ; **B262** (1991) 477.

[32] R. Barbieri and M. Frigeni, *Phys. Lett.* **B258** (1991) 395; M. Drees and M.M. Nojiri, *Phys. Rev.* **D45** (1992) 2482.

[33] R. Hempfling and A.H. Hoang, *Phys. Lett.* **B331** (1994) 99.

[34] P.H. Chankowski, S. Pokorski and J. Rosiek, *Phys. Lett.* **B274** (1992) 191; *Nucl. Phys.* **B423** (1994) 437 ; A. Brignole, *Phys. Lett.* **B281** (1992) 284; A. Yamada, *Phys. Lett.* **B263** (1991) 233 ; *Z. Phys.* **C61** (1994) 247; A. Dabelstein, *Z. Phys.* **C67** (1995) 495; D.M. Pierce, J.A. Bagger, K. Matchev and R. Zhang, *Nucl. Phys.* **B491** (1997) 3.

[35] R. Barbieri, M. Frigeni and F. Caravaglios, *Phys. Lett.* **B258** (1991) 167; Y. Okada, M. Yamaguchi and T. Yanagida, *Phys. Lett.* **B262** (1991) 54; D.M. Pierce, A. Papadopoulos and S. Johnson, *Phys. Rev. Lett.* **68** (1992) 3678; P.H. Chankowski, S. Pokorski and J. Rosiek, *Phys. Lett.* **B281** (1992) 100; K. Sasaki, M. Carena and C.E.M. Wagner, *Nucl. Phys.* **B381** (1992) 66; H.E. Haber and R. Hempfling, *Phys. Rev.* **D48** (1993) 4280; J. Kodaira, Y. Yasui and K. Sasaki, *Phys. Rev.* **D50** (1994) 7035.

[36] J.R. Espinosa and M. Quirós, *Phys. Lett.* **B266** (1991) 389.

[37] J.A. Casas, J.R. Espinosa, M. Quirós and A. Riotto, *Nucl. Phys.* **B436** (1995) 3.

[38] M. Carena, J.R. Espinosa, M. Quirós and C.E.M. Wagner, *Phys. Lett.* **B355** (1995) 209.

[39] M. Carena, M. Quirós and C.E.M. Wagner, *Nucl. Phys.* **B461** (1996) 407.

[40] H.E. Haber, R. Hempfling and A.H. Hoang, *Z. Phys.* **C75** (1997) 539.

[41] M. Schmitt, in *Supersymmetry Part II (Experiment)*, in the Particle Data Group mini-review, 1997 off-year partial update for the 1998 edition (URL: http://pdg.lbl.gov/)

[42] A. Sopczak, Karlsruhe preprint IEKP-KA-97-14 (1997) [hep-ph/9712283].